Ultra-thin PtFe-nanowires as durable electrocatalysts for fuel cells

2011 Nanotechnology 22 015602

(http://iopscience.iop.org/0957-4484/22/1/015602)

Nanotechnology **22** (2011) 015602 (5pp) doi:10.1088/0957-4484/22/1/015602

Ultra-thin PtFe-nanowires as durable electrocatalysts for fuel cells

Zhiyong Zhang[1], Meijun Li[2], Zili Wu[2] and Wenzhen Li[1]

[1] Department of Chemical Engineering, Michigan Technological University, Houghton, MI 49931, USA
[2] Center for Nanophase Materials Sciences and Chemical Science Division, Oak Ridge National Laboratory, Oak Ridge, TN 37831, USA

E-mail: wzli@mtu.edu

Received 12 September 2010, in final form 2 November 2010
Published 6 December 2010
Online at stacks.iop.org/Nano/22/015602

Abstract

Ultra-thin Pt_xFe_y-nanowires (Pt_xFe_y-NWs) with a diameter of 2–3 nm were successfully prepared through a solution-phase reduction method at Pt–Fe compositions from 1:1 to 2:1. The carbon supported Pt_xFe_y-NWs (Pt_xFe_y-NWs/C) demonstrated higher oxygen reduction reaction (ORR) activity and better electrochemical durability than conventional Pt/C catalyst. After 1000 cycles of 0–1.3 V (versus RHE), the relative electrochemical surface area (ECSA) of Pt_2Fe_1-NW/C dropped down to 46%, which was two times better than Pt/C catalyst, and the mass activity at 0.85 V (versus RHE) for Pt_1Fe_1-NW/C was 39.9 mA mg^{-1}-$_{Pt}$, which is twice that for Pt/C (18.6 mA mg^{-1}-$_{Pt}$).

(Some figures in this article are in colour only in the electronic version)

1. Introduction

Proton exchange membrane fuel cells (PEMFCs) are considered a promising alternative power source, due to their unique advantages, such as high energy conversion efficiency, environmentally benign and quick start [1, 2]. However, large-scale applications of PEMFCs are seriously hampered, due not only to high loading of expensive Pt catalysts (i.e. >0.4 mg_{Pt} $cm^{-2}_{electrode}$) [3, 4], but also to poor catalyst durability [5–7]. Coarsening of Pt nanoparticles has been identified as a serious issue under critical PEMFC operation conditions, the reduction of the electrochemical surface area (ECSA) of Pt catalysts leads to deterioration in overall PEMFC performance [6, 7].

Highly corrosion-resistant carbon nanotubes and graphitized carbon have been reported to be able to effectively anchor Pt nanoparticles from agglomeration [8, 9]. Bimetallic alloy catalysts were also found to improve the durability of Pt catalysts [10–13]. For example, PtAu/C catalysts have demonstrated much higher durability than Pt/C under potential cycling tests [11]. Recently, one-dimensional (1D) nanostructures have been emerging as a new approach to avoid agglomerations of 0D nanoparticles. For example, Pt nanotubes with a diameter of 50 nm, wall thickness of 4–7 nm, and length of 1–5 μm were reported to have super-high durability [14]: >80% ECSA survived after an accelerated durability test, while the ECSA of Pt/C dropped down to 10%. However, their small ECSA (<15 m^2 g^{-1}) due to their larger wall thickness of >4 nm and inaccessible inner tube surface area, greatly limits the oxygen reduction reaction (ORR) mass activity enhancement.

Recently, we developed a novel solution-phase reduction method to precisely synthesize PdFe-nanorods for highly active ORR catalysts [15]. In this study, we report that ultra-thin PtFe alloy-nanowires (diameter: 2–3 nm) with a large surface area (52 m^2 g^{-1}) demonstrate better durability than the commercial Pt/C catalyst in a three-compartment-cell test. Meanwhile, the PtFe-NW/C has also demonstrated better ORR activity than commercial Pt/C both before and after the durability test.

2. Experimental details

2.1. Synthesis of Pt_xFe_y-NWs

The synthesis procedures of Pt_1Fe_1-NWs are described as follows [15, 16]: a mixture of 197 mg $Pt(acac)_2$ (0.5 mmol, Acros Organics) and 20 ml oleylamine was quickly heated to 120 °C under a blanket of nitrogen and held for 30 min. After 120 μl $Fe(CO)_5$ (1.0 mmol, Acros Organics) was injected

into the synthesis system, the temperature was then raised to 160 °C and held for 30 min. The solution was cooled down to room temperature by removing the mantle heater. A mixture of 10 ml hexane and 50 ml ethanol was added and the product was separated by centrifugation (8000 rpm for 10 min). The product was cleaned by redispersing in a mixture of 5 ml hexane and 25 ml ethanol and separating by centrifugation three times. The final Pt_1Fe_1-NW (Pt–Fe atomic ratio: 1:1) sample was stored in 10 ml hexane. Following similar procedures, 60 μl (0.5 mmol) and 24 μl $Fe(CO)_5$ (0.2 mmol) were injected to prepare Pt_2Fe_1-NW and Pt_5Fe_1-NW, respectively.

2.2. Physical characterizations

The morphology and structure of the Pt_xFe_y-NWs were analyzed by Z-contrast transmission electron microscopy (Hitachi HD2000 STEM) at the Center for Nanophase Materials Sciences of Oak Ridge National Laboratory. The compositions of Pt_xFe_y-NWs were determined by energy dispersive x-ray spectroscopy (EDX) connected to a JEOL JEM-4000JX TEM instrument with an operating voltage of 200 kV. XRD patterns of the Pt_xFe_y-NWs were collected by a Scintag XDS-2000 θ/θ diffractometer with Cu Kα radiation ($\lambda = 1.5406$ Å), the tube current is 35 mA and tube voltage is 45 kV.

2.3. Electrochemical characterizations

A conventional three-compartment-cell setup (AFCELL3, Pine Instrument) with a glassy carbon working electrode (GCE), a reversible hydrogen reference electrode (Hydroflex®) and a Pt mesh counter electrode, was used for cyclic voltammetry (CV)-based durability and rotating disc electrode (RDE)-based ORR activity tests of the Pt_xFe_y-NW and Pt/C (20 wt%, E-TEK) samples at room temperature. Before testing, 1 mg of Pt_xFe_y-NWs colloidal (in hexane) was deposited on 4 mg carbon black ink (in ethanol) to make Pt_xFe_y-NWs/C catalysts. Then 1 mg catalysts were further dispersed in 1 ml ethanol and ultrasonically treated for 5 min to make a uniformed ink. The working electrode was prepared by dropping 20 μl of the ink on the glassy carbon electrode, subsequently covered by a 10 μl of 0.05 wt% Nafion. For the Pt/C, 20 μl of the ink with 1 mg catalyst/ml ethanol was used. 1000 cycles from 0 to 1.3 V (versus RHE) were performed on the electrocatalysts in 0.5 M H_2SO_4, at 50 mV s^{-1}. The ECSA was calculated based on the hydrogen desorption peak [17] and relative ECSA loss was plotted as a function of cycling number. The ORR performances on these catalysts were measured in 0.5 M H_2SO_4. The mass activities were reported at 2500 rpm and 0.85 V (versus RHE) for both Pt_xFe_y-NWs/C and Pt/C.

3. Results and discussion

3.1. Physical characterizations

The chemical compositions of Pt:Fe in the Pt_xFe_y-NWs determined by EDX are 0.8:1, 2.4:1, and 4.0:1 for Pt_1Fe_1, Pt_2Fe_1, and Pt_5Fe_1-NWs, respectively. It is interesting to find that the initially injected $Fe(CO)_5$ was only partially incorporated into the Pt_xFe_y-NWs, which is due to the evaporation of a portion of the $Fe(CO)_5$ under the nucleation temperature of 120 and ageing temperature of 160 °C, which are higher than its boiling point of 104 °C [16, 18].

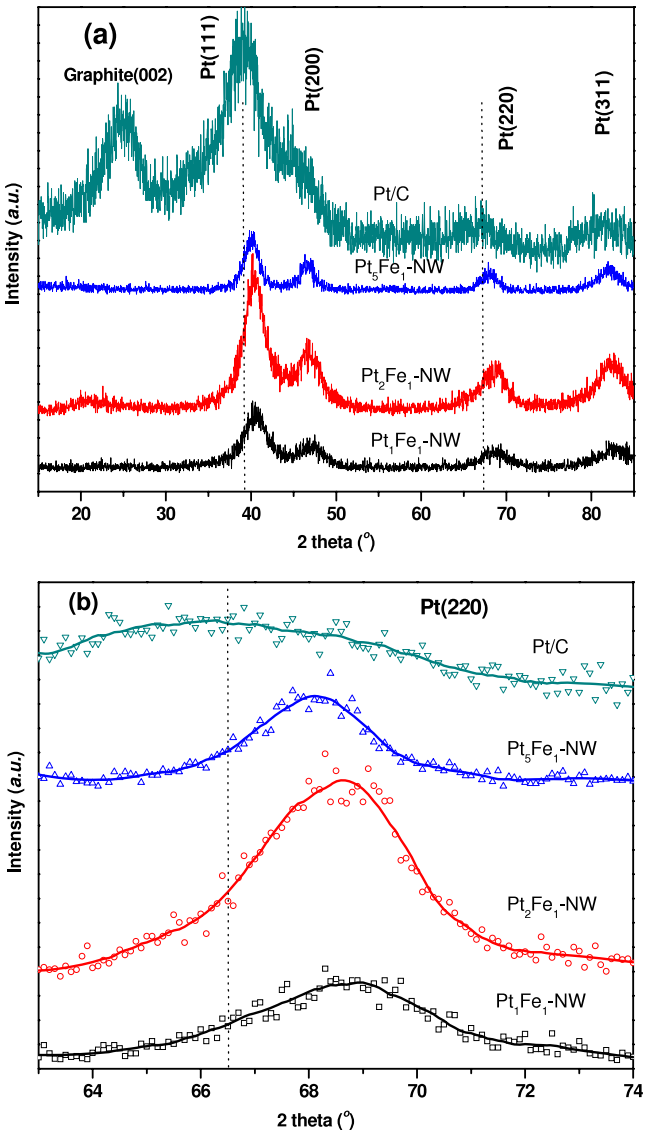

Figure 1. (a) XRD patterns of Pt_xFe_y-NWs (1:1, 2:1, 5:1) and Pt/C catalyst, (b) detailed Pt(220) diffraction peaks.

The powder XRD patterns of Pt_xFe_y-NWs and Pt/C are shown in figure 1(a). The diffraction peaks at $2\theta = 39.7°$, 46.2°, 67.3° and 81.2° are assigned to Pt(111), (200), (220) and (311) diffraction peaks, respectively, while the peak at 25.1° in the Pt/C pattern is attributed to the (002) graphitic face of carbon. No Fe diffraction peaks have been found in the XRD pattern, which indicates that the Fe have formed alloy or are in amorphous oxide states [17, 19, 20]. The average metal crystal sizes of commercial Pt/C and as-prepared Pt_xFe_y-NWs are calculated based on the Scherrer formula [17, 19–23]:

$$L = \frac{0.9\lambda_{K\alpha}}{B_{2\theta}\cos\theta_{max}} \quad (1)$$

where L is the mean crystal size, λ is the wavelength of the x-ray (1.5406 Å), B is the full width at half-maximum of the peak (rad) and θ_{max} is the Bragg angle (deg). The results yielded from the (220) peaks for Pt/C, Pt_5Fe_1, Pt_2Fe_1, and Pt_1Fe_1-nanowires are 1.8, 4.2, 3.0 and 2.6 nm, respectively. As the Fe amount in the catalysts increases, the diffraction peaks shift to the right (marked by the dashed lines for the (111) and (220) peaks in figures 1(a) and (b)). The lattice parameters of Pt/C and Pt_xFe_y-NWs were calculated from the Pt(220) diffraction peaks, and are 3.924, 3.902, 3.882, 3.871 Å for Pt/C, Pt_5Fe_1, Pt_2Fe_1, Pt_1Fe_1, respectively, showing the formation of better PtFe alloy structure with the Fe amount increasing in the catalysts. It is interesting to point out that the lattice parameter of Pt_1Fe_1-NWs is very close to that of Pt_1Fe_1 solid solution (3.877 Å, PDF 29-717), indicating a formation of ideal solution phase in these nanowires.

Typical TEM images of Pt_xFe_y-NWs are shown in figure 2. It can be found that Pt_xFe_y-NWs can be successfully synthesized in a Pt–Fe composition range of 1:1–2:1. The average diameters are 2.7 nm for Pt_1Fe_1-NW and 2.9 nm for Pt_2Fe_1-NW, which are in good agreement with the XRD results. Because the Pt_xFe_y-NWs are not straight, it is not easy to measure their length. However, when comparing figures 2(a) and (b), it is quite obvious that with Fe amount decreasing, the nanowires become shorter and thicker. When the atom ratio of Pt:Fe further increases to 5 to 1, the majority of the nanostructures are particles, and a minority short rods (shown in figure 2(c)). The Pt_5Fe_1 nanostructures have an average diameter of 4.2 nm with a broad size distribution. Comparing the TEM images of the three samples leads to a conclusion that the Fe amount in this synthesis plays a critical role on the shape and size of the products. At higher Fe amounts, long and thin nanowires can be predominantly produced, while at low Fe amounts, the major products are larger nanoparticles. In the synthesis process, OAm works as solvent, surfactant, and reducing agent, and self-organizes into elongated reverse-micelle-like structure [4], with a higher density of surfactant on the sides of Pt_xFe_y-NWs, and little on tips and ends. Therefore, Pt and Fe atoms are more likely to attached/added on the tips and ends, leading to the formation of nanowire structure. An Fe atom is likely to couple with Pt through a spin–orbit coupling and hybridization between Fe 3d and Pt 5d, and incorporated into Pt fcc crystalline structure to form a uniform phase [16]. This incorporation of Fe into the Pt crystalline structure is also evidenced by the XRD pattern, by the shift of the Pt diffraction peak to higher 2θ angle and the disappearance of the Fe diffraction peak. Reducing the amount of Fe will affect the coupling between Pt and Fe, thus changing the morphology of Pt_xFe_y-NWs [18].

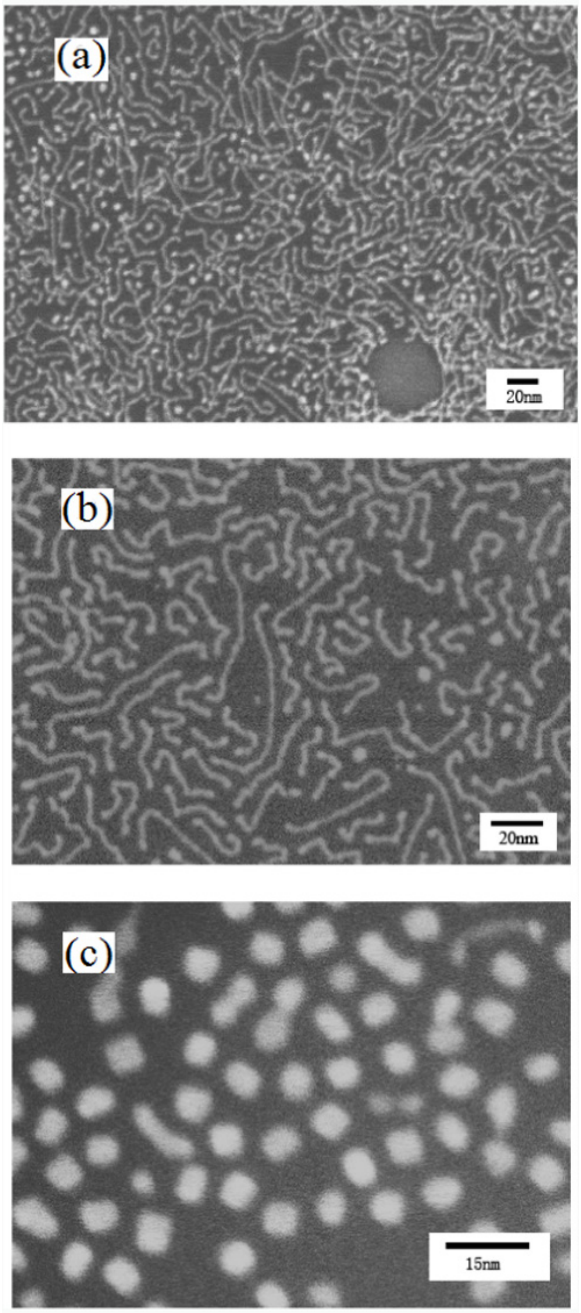

Figure 2. TEM images of (a) Pt_1Fe_1-NW; (b) Pt_2Fe_1-NW; (c) Pt_5Fe_1-NW.

3.2. Electrochemical characterizations

The durabilities of Pt_xFe_y-NWs and Pt/C catalysts were evaluated by CV-based tests. The electrochemical surface area (ECSA) was calculated from the hydrogen desorption region by the following equation [23]:

$$S_e = \frac{Q_r}{m \times C} \quad (2)$$

where m is the mass loading for Pt, Q_r is the H_2 under potential desorption charge and C is a constant (0.21 mC cm^{-2} for Pt polycrystals). The relative ECSA losses are plotted in figure 3(a) with the original ECSAs of Pt_1Fe_1-NW/C, Pt_2Fe_1-NW/C, Pt_5Fe_1-NW/C and Pt/C of 52.2, 45.6, 38.5, and 61.4 $m^2\ g^{-1}$, respectively. Although the commercial Pt/C possesses a better initial ECSA, it is noted that the Pt utilization is 76% for Pt_1Fe_1-NW/C, which is nearly twice that of Pt/C (40%). Because the CV scan of 0–1.3 V is a big challenge to Pt (the redox potential of Pt/Pt^{2+} is 1.19 V), the ECSAs of all catalysts decrease with cycling, due to the

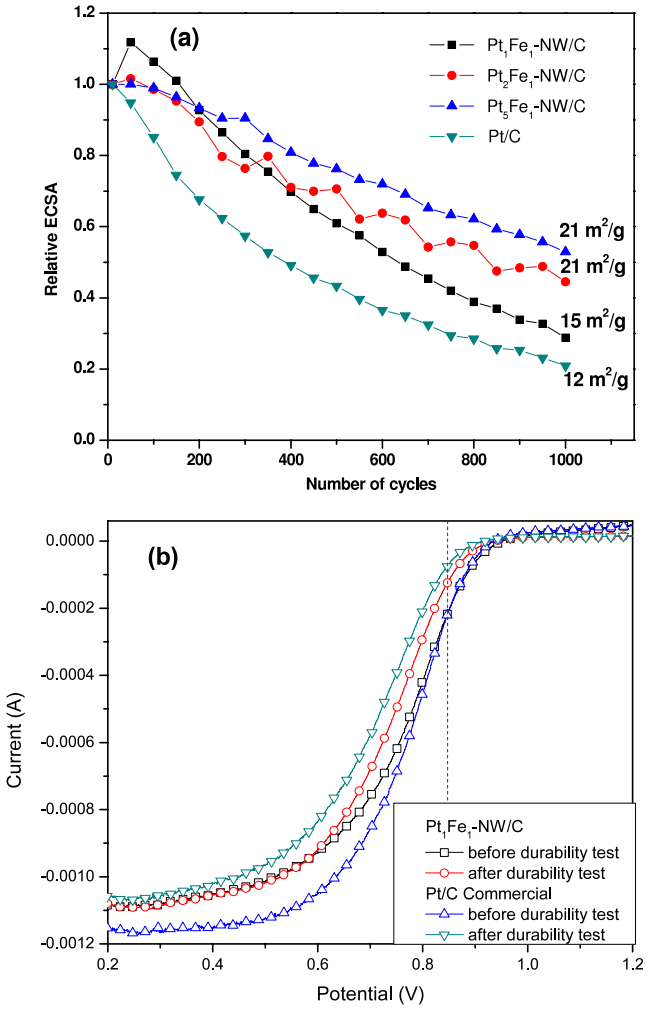

Figure 3. (a) Accelerated durability tests on Pt_xFe_y-NW(1:1, 2:1, 5:1)/C and Pt/C catalysts in 0.5 M H_2SO_4, 0–1.3 V versus RHE. Surviving ECSAs after 1000 cycles are listed on the right side. (b) ORR polarization curves of Pt_1Fe_1-NWs and commercial Pt/C catalysts before and after the accelerated durability test. Test conditions: 0.5 M H_2SO_4, 2500 rpm, room temperature.

aggregation and dissolution of Pt nanostructures [7]. However, after 1000 cycles, the relative ECSA loss of Pt_xFe_y-NWs/C is less than that for Pt/C catalysts. The absolute ECSA of Pt_2Fe_1-NW/C after 1000 cycles remains 21 m^2 g^{-1} (46% of its original ECSA), which is nearly twice that of the Pt/C catalyst (12 m^2 g^{-1}, 20% of its original ECSA). It is interesting to find that Pt_1Fe_1-NW/C has a remarkable increase in ECSA within the first 150 cycles. This is probably because long nanowires break into small units due to their very large aspect ratio, thus leading to the increase of total surface area. This trend can also be observed in the Pt_2Fe_1-NW/C sample, which also has a small increase at around 50 cycles. The better durability of Pt_xFe_y-NWs/C may lie in two possible reasons. (1) The nanowire samples have a very large aspect ratio compared to Pt/C catalysts. Therefore, the nanowires do not easily aggregate as nanoparticles, which has been identified a major cause of the surface area reduction for nanoparticle (0D sphere) electrocatalysts [7]. (2) The spin–orbit coupling and the hybridization of between Fe 3d and Pt 5d states will lead to an enhancement of the chemical stability of PtFe alloy [16, 18], and further result in the durability improvement of Pt_xFe_y-NWs.

Meanwhile, Pt_xFe_y-NWs/C catalysts also exhibit higher ORR activity when compared with that of commercial Pt/C catalysts in the course of the durability test. The ORR polarization curves of Pt_1Fe_1-NWs/C and Pt/C catalysts are shown in figure 3(b). The initial onset potential of Pt_1Fe_1-NWs is 0.95 V, which is 0.02 V lower than that of commercial Pt/C, while after the durability test, the onset potential of Pt_1Fe_1-NWs/C is still lower than that of Pt/C, indicating a better catalytic property of Pt_1Fe_1-NWs/C towards ORR reaction excited throughout the durability test. The enhanced ORR activity of Pt_1Fe_1-NWs/C can also be proved by the kinetic currents (i_k) calculated by equation (3), which is derived from the Levich–Koutecky equation [24]:

$$i_k = \frac{i \times i_d}{i_d - i} \tag{3}$$

where the diffusion limiting currents (i_d) were collected at the region below 0.3 V, and the currents (i) were directly obtained from the polarization curves. After normalizing the kinetic currents with the metal loading, Pt_1Fe_1-NWs/C shows a mass activity (M.A.) of 77.1 mA mg^{-1}_{Pt} at 0.85 V, while that of Pt/C was 65.7 mA mg^{-1}_{Pt}. After the durability test, the M.A. of Pt_1Fe_1-NWs/C only decreased to 39.9 mA mg^{-1}_{Pt}, which is twice that of Pt/C (18.6 mA mg^{-1}_{Pt}). The calculation of M.A. shows that Pt_xFe_y-NWs/C possesses both a higher ORR activity and a better electrochemical durability than commercial Pt/C catalysts. While the better durability can be attributed to the high aspect ratio 1D nanowire structure and the spin–orbit coupling and hybridization between Fe and Pt, the reasons for the better ORR activity may arise from the electronic effects. It is well known that the ORR activity can be enhanced through the modified electronic structure of the Pt surface layer by the underlying M (Fe, Ni, Co, etc) sub-layer [3, 25–27]. The surface transition metal Fe has a redox potential much lower than the precious metal Pt, which will leach out under electrochemical cycling, and could lead to the formation of Pt-rich shell nanostructures. The adsorption energy of oxygen on surface Pt will be reduced by the sub-layer Fe atoms, resulting in a better ORR activity than that of commercial Pt/C catalyst. In order to acquire a better understanding of the mechanisms, research efforts on detailed characterizations of the nanowire samples are currently underway.

4. Conclusions

In this study, ultra-thin Pt_xFe_y-NWs were successfully prepared through a solution-phase reduction route. The Pt_xFe_y-NWs/C have higher electrochemical surface areas and Pt utilization (i.e. 52 m^2 g^{-1} and 76% for Pt_1Fe_1-NW/C). They can survive better than Pt/C under accelerated electrochemical cycling tests. It is very interesting to find that Pt_xFe_y-NWs have an enhanced intrinsic ORR activity compared to commercial Pt/C. Therefore, the ultra-thin nanowires show great potential as promising fuel cell electrocatalysts.

Acknowledgments

This work is supported by ACS-PRF-DNI and NSF-CBET 1032547. A portion of this research was conducted at the Center for Nanophase Materials Sciences, which is sponsored at Oak Ridge National Laboratory by the Division of Scientific User Facilities, US Department of Energy. The research was supported in part by the appointment for M J Li to the ORNL Research Associates Program, administered jointly by ORNL and the Oak Ridge Associated Universities.

References

[1] Dresselhaus M S and Thomas I L 2001 *Nature* **414** 332–7
[2] Vielstich W, Lamm A and Gasteiger H A 2003 *Handbook of Fuel Cells: Fundamentals, Technology, Applications* (New York: Wiley)
[3] Gasteiger H A, Kocha S S, Sompalli B and Wagner F T 2005 *Appl. Catal.* B **56** 9–35
[4] Mathias M F *et al* 2005 *Interface* **24** 24–35
[5] Borup R *et al* 2007 *Chem. Rev.* **107** 3904–51
[6] Jian X, Wood D L, More K L, Atanassov P and Borup R L 2005 *J. Electrochem. Soc.* **152** A1011–20
[7] Ferreira P J, la O G J, Shao-Horn Y, Morgan D, Makharia R, Kocha S and Gasteiger H A 2005 *J. Electrochem. Soc.* **152** A2256–71
[8] Wang X, Li W Z, Chen Z W, Waje M and Yan Y S 2006 *J. Power Sources* **158** 154–9
[9] Yano H, Akiyama T, Bele P, Uchida H and Watanabe M 2010 *Phys. Chem. Chem. Phys.* **12** 3806–14
[10] Gonzalez E R, Antolini E and Salgado J R C 2006 *J. Power Sources* **160** 957–68
[11] Zhang J, Sasaki K, Sutter E and Adzic R R 2007 *Science* **315** 220–2
[12] Peng Z M and Yang H 2009 *J. Am. Chem. Soc.* **131** 7542
[13] Zhou Z M, Shao Z G, Qin X P, Chen X G, Wei Z D and Yi B L 2010 *Int. J. Hydrog. Energy* **35** 1719–26
[14] Chen Z W, Waje M, Li W Z and Yan Y S 2007 *Angew. Chem. Int. Edn* **46** 4060–3
[15] Li W Z and Haldar P 2009 *Electrochem. Commun.* **11** 1195–8
[16] Wang C, Hou Y L, Kim J M and Sun S H 2007 *Angew. Chem. Int. Edn* **46** 6333–5
[17] Li W Z, Xin Q and Yan Y S 2010 *Int. J. Hydrog. Energy* **35** 2530–8
[18] Sun S H, Fullerton E E, Weller D and Murray C B 2001 *IEEE Trans. Magn.* **37** 1239–43
[19] Li W Z, Liang C H, Qiu J S, Li H Q, Zhou W J, Sun G Q and Xin Q 2004 *React. Kinet. Catal.* L **82** 235–40
[20] Li W Z, Zhou W J, Li H Q, Zhou Z H, Zhou B, Sun G Q and Xin Q 2004 *Electrochim. Acta* **49** 1045–55
[21] Li W Z, Liang C H, Qiu J S, Zhou W J, Han H M, Wei Z B, Sun G Q and Xin Q 2002 *Carbon* **40** 791–4
[22] Li W Z, Liang C H, Zhou W J, Qiu J S, Zhou Z H, Sun G Q and Xin Q 2003 *J. Phys. Chem.* B **107** 6292–9
[23] Hsu R S, Higgins D and Zhongwei C 2010 *Nanotechnology* **21** 165705
[24] Paulus U A, Wokaun A, Scherer G G, Schmidt T J, Stamenkovic V, Radmilovic V, Markovic N M and Ross P N 2002 *J. Phys. Chem.* B **106** 4181–91
[25] Toda T, Igarashi H, Uchida H and Watanabe M 1999 *J. Electrochem. Soc.* **146** 3750–6
[26] Stamenkovic V R, Fowler B, Mun B S, Wang G F, Ross P N, Lucas C A and Markovic N M 2007 *Science* **315** 493–7
[27] Li W Z and Haldar P 2010 *Electrochem. Solid State Lett.* **13** B47–9